Molecular and functional characterization of VDAC2 purified from mammal spermatozoa

Viviana Andrea Menzel, Maria Carolina Cassarà, Roland Benz, Vito de Pinto, Angela Messina, Vincenzo Cunsolo, Rosaria Saletti, Klaus Dieter Hinsch, Elvira Hinsch

MOLECULAR AND FUNCTIONAL CHARACTERIZATION OF VDAC2 PURIFIED FROM MAMMAL SPERMATOZOA*

Viviana Andrea Menzel[#], Maria Carolina Cassarà[#], Roland Benz[§], Vito De Pinto[$,¶], Angela Messina[$], Vincenzo Cunsolo[$], Rosaria Saletti[$], Klaus Dieter Hinsch[#,*], and Elvira Hinsch[#]

[#]Center of Dermatology and Andrology, Justus Liebig University of Giessen, Gaffkystr. 14, DE-35392, Germany, [§]Lehrstuhl für Biotechnologie, Universität Würzburg, DE-97074 Würzburg, Germany, [$]Department of Chemistry, Laboratory of Biochemistry and Molecular Biology, University of Catania, IT-95125 Catania, Italy and Institute for Biomembranes and Biosystems, Roma, Italy, [*]Borkum Riff Rehabilitation Clinic of the federal insurance for salaried employees' Institution (DRV-Bund), DE-26757 Borkum, Germany

Short title: VDAC2 from spermatozoa

Keywords: VDAC2, spermatozoa, mitochondria, purification, porin isoforms, sequence analysis.

*This work was supported by funds from the Deutsche Forschungsgemeinschaft Hi 610/3-1, Hi 610/3-2, by the Fonds der Chemischen Industrie (to R.B.), and by University of Catania and FIRB RBNE03PX83 and RBRN07BMCT (to V.D.P.).

[¶]Corresponding author:
dr. Vito De Pinto
University of Catania
Dept. Chemical Sciences
v.le A. Doria, 6
IT-95125 Catania, ITALIA
Tel:. +39-0957384244
Fax: +39-095337036
E-mail: vdpbiofa@unict.it

ABSTRACT

VDAC (Voltage Dependent Anion selective Channel) is the pore-forming protein located in the outer mitochondrial membrane. In higher eukaryotes three genes encode for VDAC. Nevertheless the knowledge of VDAC isoforms is mainly restricted to VDAC1, the only isoform characterized from living tissues until now. We have highly enriched the isoform VDAC2 using as starting material bovine spermatozoa. VDAC2 was obtained in the hydroxyapatite/celite pass-through of sperm proteins solubilized with Triton X-100. This fraction showed in SDS-PAGE two major and one-faint bands in the Mr range of 30-35 kDa. Two-dimensional electrophoresis resolved these bands in ten spots with various Coomassie staining intensities. Western blot analysis with antibodies monospecific for each isoform and MS peptide sequencing showed that the main protein resolved in electrophoresis was VDAC2 with minor contaminations of the other isoforms. Proteomic analysis of the higher Mw VDAC2 protein allowed the coverage of the whole protein with the exception of the tri-peptide $A_{24}AR_{26}$. In the same material it was revealed the presence of two possible amino acid substitutions (T_{88} to L_{88} and A_{97} to Q_{97}). Reconstitution of VDAC2 pores in planar lipid bilayers showed typical features of mitochondrial porins. Step-wise increases in membrane conductance were observed with a predominant conductance of about 3.5 nS in 1 M KCl. Very often small short-lived fluctuations were observed with single-channel conductance of about 1.5 nS. Bovine spermatozoa VDAC2 was anion-selective and showed voltage dependence. This is the first work reporting the purification and characterization of VDAC2 from a mammalian tissue.

INTRODUCTION

Voltage-dependent anion channels (VDACs), also known as mitochondrial porins, are the most abundant integral membrane proteins found in the outer membrane, separating the intermembrane space from the cytosol [1-2]. They are pore-forming proteins (30-35 kDa) originally identified in mitochondria of eukaryotic cells [1]. Functional characterization of these proteins has been mainly achieved by reconstitution into planar bilayer membranes [for review see 2]. The pore incorporated in the membrane shows current increases with a predominant single channel conductance of about 4nS (in 1M KCl) and a slight preference for anions over cations (2:1). VDAC displays sensitive voltage dependence when assayed under in vitro conditions. At low voltages, the channel exists in its full open state (with a diameter of ~3nm) and upon application of voltages larger than 20 mV, it switches to subconducting states. In these subconducting states, VDAC has a reduced permeability and a reversed selectivity [3].

An increasing body of evidence indicates that VDAC plays a major role in the metabolite flow in and out of mitochondria resulting in the regulation of mitochondrial functions [4]. The whole exchange of metabolites and information between mitochondria and the cell occurs through the outer membrane. This membrane creates a diffusion barrier for small molecules (adenine nucleotides, creatine phosphate, creatine etc.) causing rate-dependent concentration gradients as a prerequisite for the action of ADP shuttles via creatine kinases or adenylate kinases. This means that VDAC, as a consequence of closing and opening, may act as a „governor“ of the mitochondrial bioenergetics [5].

VDACs have also been described in association with apoptotic processes and interacting with cytoskeletal proteins [4-8]. Although VDACs were originally thought to be located exclusively in the outer mitochondrial membrane, several investigations demonstrated their presence in other cell compartments, e.g. nuclear envelope, endosomes, sarcoplasmatic/endoplasmatic reticulum, plasma membrane [for reviews see 4, 9].

In the evolution VDACs developed as slightly basic proteins with Mr around 30 kDa and a structural organization as β-barrel cylinder [10]. Gene duplication or other evolutionary events originated sets of porin genes in almost any organism studied so far. In mammals three different VDAC genes encode three proteins whose sequences are homologous [11]. Functional experiments demonstrated that recombinant VDAC1 and VDAC2 isoforms are able to form pores in lipid bilayers, but recombinant VDAC3 has no evident pore-forming ability [12]. Human and mouse recombinant VDAC1 and VDAC2 isoforms can complement the yeast VDAC1 deficiency, while VDAC3 cannot complement this defect [11]. VDAC deficient mice have been obtained. VDAC1 deficient mice are viable and show that mitochondrial functions are slightly affected; VDAC2 gene deletion is lethal [13]; mice lacking VDAC3 are healthy, but males are infertile [14]. Mammalian VDAC isoforms are expressed in a wide variety of tissues; the specific expression of VDAC3 was observed in mammalian testes [15]. Each VDAC isoforms may thus have some distinct physiological role.

In comparison with the most abundant isoform VDAC1, there is little knowledge about the functional role of the other isoforms VDAC2 and VDAC3. In addition, the existing information derives mainly from recombinant proteins expressed in yeast or *E. coli* and from mutant mice and cells [16]. This is due to the fact that until now only VDAC1 has been purified and characterized from animal tissues.

Recent investigations gave interesting insight in the role of VDAC2 in the physiology of the cell. In a report from the Korsmeyer group, it was found that VDAC2 can exert a protective effect over the onset of mitochondrial apoptosis [13]. Triggering the activation of the multidomain death effectors Bax and Bak resulted in the permeabilization of the mitochondrial outer membrane and the release of pro-apoptotic proteins including cytochrome c. Cheng et coworkers discovered that Bak in the

mitochondria of viable cells is present in complex with VDAC2 [13]. Re-expressing VDAC2 in *VDAC2–/–* ES cells by retroviral transduction restored the 60-kDa complex. The authors showed several experimental evidence pointing to the relevant consideration that a distinctive physiological role *in vivo* for the VDAC2 isoform could be as a specific inhibitor of Bak-dependent mitochondrial apoptosis. This conclusion suggests that, as Bcl-2 proapoptotic effectors expanded in number and complexity, a physiological component of the mitochondrial membrane, VDAC2, coevolved to regulate cell death. The interaction of VDAC2 with Bak was confirmed by Chandra et al [17] that described its regulation by Bax.
Furthermore, using affinity purification and mass spectrometry, Yagoda et al discovered that erastin, a new anti-cancer compound, acts through mitochondrial voltage-dependent anion channels [18]. Erastin treatment of cells harbouring oncogenic RAS causes the appearance of oxidative species and subsequent death through an oxidative mechanism [18]. They found that erastin alters the permeability of the outer mitochondrial membrane in purified mitochondria expressing a single VDAC isoform. Using a radiolabelled analogue and a filter-binding assay, they showed that erastin binds directly to VDAC2 [18].

In previous studies we reported the presence of VDAC isoforms in the outer dense fibers (ODF) of the bovine sperm flagellum [15]. Their involvement in the regulation of essential sperm functions was also shown [19]. Further evidence for the presence and function of VDAC in spermatozoa has been also showed elsewhere [14, 20].
In the present study, we describe for the first time a purification protocol from mammalian spermatozoa resulting in a fraction highly enriched in VDAC2. The isolated protein was characterized by proteomic and immunological methods with subtype-specific anti-VDAC antibodies [15]. Furthermore, the channel-activity and the molecular structure of the purified VDAC2 was analyzed.

MATERIALS AND METHODS

Protein Extraction and Purification. Bovine ejaculates [15] were washed in PBS to separate spermatozoa from the seminal plasma. The spermatozoa were resuspended in 2% Triton X-100 extraction buffer (150 mM NaCl; 50 mM Tris-HCl, pH 7.4; 2 mM DTT; 1 mM EDTA; 10 mM benzamidine; 0.2 mM PMSF) at a concentration of 330 x 10^6 cells/ml. The suspension was incubated for 1 h at 4°C, finally centrifuged at 6000 g for 30 min, and the supernatant was stored at –80°C until use. Proteins from 165 x 10^6 cells in 1 ml 2% Triton X-100 extraction buffer were applied to a dry hydroxyapatite/celite (2:1 w/w, H/C) column [21]. The first ml of the pass-through (VDAC-containing fraction) was collected and stored at –20°C until use.

Protein Detection by Western Blotting. Total protein extract (2% TX-100) and purified VDAC (H/C) were precipitated with ice-cold acetone by centrifugation at 6000 x g and 4°C for 30 min. Proteins were resuspended in sample buffer and SDS-PAGE was performed according to Laemmli [22] in 12% (v/v) polyacrylamide gels. 2% Trition X-100 extracts from 25 x 10^6 spermatozoa or H/C from 165 x 10^6 cells were loaded per lane.
Gels were subjected to Coomassie Simply Blue Safe Stain (Invitrogen) or to western blotting [23]. After protein transfer to nitrocellulose membrane, immuno blotting using specific anti-VDAC antisera was performed as previously described [15]. The antibodies used were AS P6 (anti-VDAC1), AS P2/45 (anti-VDAC2), AS P3/31 (anti-VDAC3) at appropriate dilutions [15].

Protein Detection after Two-Dimensional Gel Electrophoresis (2-DE). VDAC H/C extracts were solubilized in IPG buffer (8 M urea; 2% w/v CHAPS; 18 mM DTT; 0.5% w/v carrier ampholytes and traces of bromophenol blue) and loaded onto IPG strips (pH 6-11, 7 cm, Amersham). Extracts from 330 x 10^6 spermatozoa were loaded for subsequent western blot and from 412.5 x 10^6 cells for protein staining. The isoelectric focusing (IEF) was programmed with the linear ramping method: S1 250 V, 15 min; S2 4000 V, 2h; S3 4000 V - 15000 V. After IEF, proteins were S-alkylated. IPG strips were allowed to equilibrate with two incubations, 10min each, in the equilibration solution (6 M urea; 20% v/v glycerol; 2% w/v SDS; 0.05 M Tris-HCl, pH 8.8) containing 2% w/v DTT (first incubation) then 2.5% w/v iodoacetamide (second incubation), at room temperature. The IPG strips were directly applied to the top of 12% SDS-PAGE gels and run at 200 V according to Laemmli [22]. Proteins were visualized by Coomassie SimplyBlue Safe staining or subjected to western blotting as described above.

Protein Identification by Mass Spectrometry.

Trypsin in-gel digestion. The investigated bands or spots were excised from the SDS gel, washed, in-gel reduced by DTT, S-alkylated with iodoacetamide, and subjected to in-gel trypsin digestion according to Shevchenko et al [24]. The gel pieces were swollen in a digestion buffer containing 50 mM NH_4HCO_3 and 12.5 ng/μL trypsin (modified porcine trypsin, sequencing grade, Promega, Madison, WI) in an ice bath. After 30 min the supernatant, containing excess trypsin, was removed and discarded and 50 μL of 50 mM NH_4HCO_3 was added to the gel pieces. Digestion was allowed to proceed at 37°C overnight. The enzymatic reaction was stopped cooling the gel pieces and supernatant solution at -24°C.

MALDI-TOF MS analysis. 10 μL of the supernatant solution containing tryptic peptides were used for micro-purification (desalting/concentration) of peptides with a homemade 5-mm nanocolumn packed with C18 resin (POROS R2) (Applied Biosystems, Foster City, CA, USA) in a constricted GELoader tip (Eppendorf Scientific, Westbury, NY), according to Gobom et al. [25] A syringe was used to force liquid through the columns by applying gentle air pressure. The columns were washed with 10 μL of 0.1 % trifluoroacetic acid (TFA) and the bound peptides subsequently eluted directly onto the MALDI target with 0.6 μL of matrix solution (10 mg/mL α–cyano-4-hydroxycinnamic acid in 70% [v/v] CH_3CN and 0.1% TFA [w/v]) and deposited directly onto the MALDI target.

MALDI mass spectra were acquired in positive ion reflectron-delayed extraction mode over a *m/z* range 600-4000, using a Voyager DE-PRO time-of-flight mass spectrometer (Applied Biosystems) equipped with UV nitrogen laser (337 nm). Typically, 150 shots were averaged to improve the S/N ratio. The *m/z* software (Proteometrics, NY) was used to analyze MS spectra. MALDI-TOF spectra were internally calibrated using porcine trypsin autolysis products (*m/z* 842.51 and 2211.10). When trypsin autolysis peaks could not be detected, bovine β-lactoglobulin tryptic peptides (*m/z* 837.48, 2313.26 and 2707.38) were used for external mass calibration. So called project-specific contaminants (peaks present in all mass spectra; mostly but not only originating from contaminating human keratin or the trypsin added for digestion of proteins) were identified and eliminated from the MS spectra using the software PeakErazor (http://www.welcome.to/GPMAW).

The General Protein/Mass Analysis for Windows (GPMAW) software (http://welcome.to/gpmaw) was used for all sequence handling and storage.

RP-HPLC/nESI-MS/MS of the in-gel tryptic digests. RP-HPLC/nESI-MS/MS of the tryptic digests were carried out on a Dionex Ultimate 3000 autosampler/LC MS-pump high-performance liquid chromatograph equipped with capillary split (1/100). 10 μL of the tryptic mixture were loaded onto a preconcentration-column and eluted with 95:5 (v/v) of solvent A (H_2O + 0.05 % Formic Acid)/solvent B (CH_3CN + 0.05% Formic Acid) for 5 min. Then, a switch system loads the concentrated mixture sample into reversed-phase Thermo BioBasic-18 column (0.18 x 150 mm, 300 Å, 5 μm). The column

was eluted at room temperature with a linear gradient of solvent B in A from 5 % to 50 % in 35 min at a flow rate of 2 μL/min. The HPLC system was interfaced to a linear ion trap nano-electrospray mass spectrometer ThermoFinnigan LTQ. Repetitive mass spectra were acquired in positive ion mode in the *m/z* range 150-2000. The amino acid sequences of the peptides of interest, detected during LC-ESI/MS, were determined by tandem mass spectrometric analysis (MS/MS). The operating conditions for MS/MS analysis were: isolation width 2, normalized collision energy about 23 %, activation Q 0.250.

Protein identification. Protein identification was performed by searching the MALDI-MS spectra against a nonredundant protein sequence database (NCBInr) *via* the MASCOT program (http://www.matrixscience.com), limited to the *mammalia* taxonomy. The following parameters were used for a standard database search: monoisotopic mass accuracy, 80 ppm; missed cleavages, 1; complete carbamidomethylation of cysteines, partial oxidation of methionines and partial transformation of *N*-terminal glutamine and *N*-terminal glutamic acid residues in the pyroglutamic acid form. For positive identification, the score of the result of (-10 × Log(P)) had to be over the significance threshold level ($p < 0.05$). In addition, significant hits were carefully inspected manually to eliminate possible false positives, based on criteria such as mass error distribution and likely/notlikely missed cleavages. To qualify as a positive identification, over 20% sequence coverage was required, including at least four independent peptides with a mass deviation of less than 60 ppm.

Reconstitution experiments. The method of reconstitution of purified VDAC protein into black lipid bilayer membranes has been previously described [26]. Briefly, membranes were formed from a 1% solution of diphytanoyl phosphatidylcholine (DiphPC, Avanti Polar Lipids, Alabaster, AL) in n-decane by painting onto a circular hole (surface area about 0.4 mm^2) separating the two compartments of a Teflon chamber. Reconstitution experiments were initiated after the lipid bilayer membrane thinned out and turned optically black to reflected light indicating bilayer formation. The aqueous salt solutions (Merck, Darmstadt, Germany) were used unbuffered and had a pH around 6. The temperature was kept at 20°C throughout. VDAC was reconstituted into the lipid bilayer membranes by adding concentrated stock solutions to the aqueous phase to one side (the *cis*-side) of a membrane in the black state. Membrane reconstitution reached its maximum between 10 to 20 min after addition of protein to the *cis* side.

The membrane current was measured with a pair of Ag/AgCl electrodes switched in series with a voltage source and an electrometer (Keithley 602). In the case of the single channel recordings the electrometer was replaced by a current amplifier. The amplified signal was monitored with a storage oscilloscope and recorded with a tape or a strip chart recorder. Zero-current membrane potential measurements were performed by establishing a salt gradient across membranes containing 100 to 1000 channels as has been described earlier [27].

RESULTS

VDAC2 extraction and purification from spermatozoa. We have recently reported about the presence of VDAC2 and VDAC3 in the ODF (Outer Dense Fiber) and, in general, in spermatozoa of bovine [15, 19]. By means of a set of monospecific anti-VDAC isoforms antibodies developed in our laboratory we could detect the presence of VDAC isoforms in bovine spermatozoa. VDAC2 and 3 are typically present in the ODF fraction while VDAC1 is present in low abundance and not in ODF [15]. Since spermatozoa are a tissue that can be isolated easily, if not in large abundance, and it looks like to be a rich source of VDAC2, we used them as starting material to try purification procedures, with the aim to isolate VDAC isoforms. The procedure adopted to purify VDAC1 from mitochondria of several

tissues [21] was adapted to the spermatozoa. Whole, fresh spermatozoa were solubilized in 2% Triton X-100. This non-ionic detergent gave an optimal extraction with respect to other detergents and was able to extract all the VDAC2 present in the cell as controlled with antibodies (not shown). The Triton X-100 protein extract was applied onto an HTP/celite chromatographic column and the elution performed with the extraction buffer. The eluted fractions were applied onto SDS-PAGE to determine the purity of the proteins. Like VDAC1 from mitochondria of other species and tissues, sperm VDAC2 was recovered in the pass-through of the column just after the void volume. The composition of this eluate was visualized by SDS-PAGE and is shown in Fig. 1. Staining of proteins with Coomassie blue resulted in 3 distinct bands with slight mobility differences around 35 kDa. Immunoblot analysis with anti-VDAC subtype specific antisera revealed that band I and II, differing of about 1-2 kDa, (Fig. 1) were detected by a monospecific antibody anti-VDAC2, while band III was identified either with anti-VDAC3 and anti-VDAC1 antibodies (not shown).

To detect differences in these bands from mono-dimensional gel electrophoresis, they were subjected to tryptic in-gel digestion and and their peptide sequences were characterized by mass spectrometry. MALDI-TOF MS and RP-HPLC/nESI-MS/MS data of the in-gel tryptic digest of the high molecular weight VDAC2 band confirms the cDNA-deduced amino acid sequence, allowing the characterization of the whole amino acid sequence (nr NCBI Acc. N. NP 776911; gi 62177148), with the exception of the short fragment Ala-Ala-Arg (Fig.1B). In addition, mass spectrometric analysis showed that the mature chain of VDAC2 does not present the methionine at position 1, but the N-terminal residue is the acetylated Ala_2. On this respect, this result represents the first extensive protein coverage of VDAC2 (sequence coverage 98.6 %), improving the previously sequence characterization performed by Distler et al. (sequence coverage 89.5 %) [28].

Moreover, RP-HPLC/ESI-MS/MS analysis allowed the detection of the doubly-charged molecular ions at *m/z* 1267.0 (M_r 2532 Da) and 1288.7 (M_r 2575.4 Da), values which do not match with any of the expected tryptic fragments of VDAC2. The signals in the MS/MS spectrum corresponding to the doubly-charged molecular ion at *m/z* 1266.0 (M_r 2530 Da) fit with the sequence WN**L**DNTLGTEIAIEDQICQGLK, which correspond to that of the tryptic peptide T_{11} (M_r 2518 Da) with the amino acid substitution Leu_{88} (Ile)→ Thr. The MS/MS data of the doubly-charged molecular ion at *m/z* 1288.7 (M_r 2575.4 Da) are instead consistent with the sequence WNTDNTLGTEI**Q**IEDQICQGLK, which correspond to that of T_{11} (M_r 2518 Da) with the amino acid substitution Gln_{97}→Ala (Fig. 1B).

The presence of these two modified peptides T_{11}, together with the presence of the unmodified T_{11}, could justify the splitting of the investigated SDS-band in more spots with different p*I* during the 2D-PAGE run (see below). It is also useful to notice that there is a substantial lack of major post-translational modifications of bovine VDAC2.

In-gel tryptic digestion and MS analysis of the low molecular weight band II allowed the coverage of 71% of the VDAC 2 amino acid sequence (nr NCBI Acc. N. NP 776911; gi 62177148). In this case, sequence coverage was scant with respect to the characterization of the high molecular weight band (Fig. 1B). Nevertheless, RP-HPLC/ESI-MS/MS data show that the protein has no methionine at position 1, and the N-terminal alanine is acetylated, as has previously been found for the high molecular weight band of VDAC2.

Two-dimensional analysis of the VDAC2 enriched fraction from spermatozoa. To fill the gaps left by the first analysis of the sequence of VDAC2, we performed 2-D gel electrophoresis of the same sample. Coomassie staining of 2-D gels revealed five distinct main protein spots (Fig. 2, 1-5), four minor spots (Fig. 2, 6-9) and one faint and relatively broad protein smear (Fig. 2, 10).

Immuno blotting of the 2-D gel was used to identify the spots. Figure 3A shows the result of the immunodetection with anti-VDAC1 antibodies. These antibodies immunodecorated four protein spots

with apparent molecular masses of about 30 kDa and *pI*s between 7 and 9. It was known since the earliest time in 2-D electrophoresis that VDAC1 is able to form a set of three close spots in the basic pH [29]. The fourth spot was not known. These spots correspond to the spots 8 and 9 stained with Coomassie (Fig. 2).

The anti-VDAC2 antibodies detected five distinct spots (Fig. 3B). Interestingly they were not arranged in the usual way. Instead they were distributed in an ordered array of five major spots corresponding to two distinct molecular weights (33-35 kDa) and three *pI*s (6 to 7.5). The Western blot suggests that these spots correspond to the major ones stained with Coomassie (Fig. 2).

Anti-VDAC3 antibodies reacted with a broad smear at a molecular mass of about 31 kDa with a *pI* of around 9 (Fig. 3C). This should correspond to the protein smear barely stained with Coomassie and indicated as 10 in Fig. 2.

The results obtained from the immunoblots were supported by sequencing of tryptic peptides from 2-D gel spots. A clear identification could be obtained in every spot with the exception of spot 7 (no peptide sequence data could be generated) and of the smear 10 (no statistical significance in protein coverage rate was calculated). Table 1 shows that the main spots 1-5 and the minor spot 6 contained peptides from VDAC2, while protein spots 8 and 9 consisted of peptides with VDAC1 sequences. The VDAC protein from smear 10 most probably represents sperm VDAC3; however, here peptide sequencing data were not significant from their rate of protein coverage. The sequence information thus completely confirmed the results obtained with immuno blotting.

Reconstitution experiments using VDAC from bovine spermatozoa. The purified VDAC was incorporated into lipid bilayer membranes to study its function. When VDAC was added in small quantities (10 to 100 ng/ml) to the aqueous phase on one or both sides of an artificial bilayer, the conductance of the membrane increased by several orders of magnitude. After a rapid increase during 15 to 20 min, the membrane conductance increased at a much slower rate. This slow increase continued usually until membrane breakage. The addition of the detergent alone in a similar concentration to that used with the protein did not lead to any appreciable change in the membrane conductance indicating that the membrane activity was caused by the protein and did not represent a detergent artefact.

Single-channel experiments. The addition of VDAC purified from bovine spermatozoa at very small concentrations (5ng/ml) to the aqueous solution on one side of an artificial lipid bilayer membrane allowed the resolution of step increases in membrane conductance (Fig. 4), each step corresponding to the incorporation of one channel-forming unit into the membrane. Many of the conductance steps had a single-channel conductance of about 3.5 nS in 1 M KCl (Fig. 5, Table 2). Very often small short-lived fluctuations were observed on top of the conductance steps (Fig. 4). The histogram of the current fluctuations demonstrated that a considerable number of conductance steps had only a single-channel conductance of about 1.5 nS (Fig. 5). Bovine spermatozoa VDAC was permeable for a variety of ions. Table 2 shows the single channel conductance for different salt solutions. Although a considerable influence of the type of ions on the pore conductance was found, the ratio between single channel conductance G and the bulk aqueous conductance varied less than a factor of two. Data of Table 2 show that the channels exhibit certain ion selectivity. The difference of the single channel conductance between potassium acetate and LiCl suggested that the channel was anion-selective.

Selectivity measurements. Selectivity measurements allow a quantification of the permeability of enriched VDAC2 pore for anions relative to cations. They were performed in multi-channel experiments under zero-current conditions in KCl. Membranes were formed in 100 mM KCl solution and enriched VDAC2 protein was added to the aqueous phase when the membranes were in the black state. After the incorporation of approximately 100 pores into the membrane, five-fold KCl gradients were established by the addition of small amounts of 3 M KCl solution to one side of the membrane.

The potential on the more diluted side of the membrane was negative under these conditions throughout the experiments. (V_m = -3.8 ± 0.2mV), suggesting preferential movement of anions through the VDAC2 pore. The permeability ratios for anions over cations through enriched VDAC2 were calculated using the Goldman-Hodgkin-Katz equation [27]. The ratio of the permeability coefficients P_{cation}/P_{anion} in KCl was 0.80 ± 0.03 indicating an only small selectivity of VDAC2 for anions. This means that also potassium ions may pass the pore at almost the same rate as chloride.

Voltage-dependence. Voltage-dependence experiments with bovine spermatozoa VDAC were performed under multi-channel conditions, i.e. many pores were reconstituted into the membrane. The voltage across the membrane was set to different potentials ranging from 10 mV to 100 mV and the membrane currents were monitored on the strip chart recorder (Fig. 6A). The initial current, i.e. the current immediately after application of the voltage, was a linear function of the applied membrane potential. For voltages larger than 20 mV the membrane current decayed exponentially to a smaller value (Fig. 6B). The maximum conductance decrease was observed at a voltage of about 70 mV. Higher potentials did not cause a further conductance decrease**.**

DISCUSSION

Voltage dependent anion selective channels (VDACs or mitochondrial porins) are important but still elusive proteins that attract the attention of several investigators due to their abundance in the outer mitochondrial membrane. The genes coding for these proteins have been studied in detail in different organisms [11, 30]. Proteomic approaches have found interesting changes in the expression of these proteins in several pathologic occurrences, ranging from Alzheimer and Down [31] to cancer [32-33]. However, until now, VDAC1 has been the only member of this family to be purified from an animal tissue and functionally characterized. This is a necessary step to understand the function of a protein and the basis of its interaction with neighbouring molecules. Because we discovered that mammal spermatozoa are especially enriched in VDAC2 and VDAC3 [15], we started a porin purification experiment using these cells. The freshly ejaculated sperms were extracted with non-ionic detergents and loaded onto a chromatographic column, containing hydroxyapatite/celite, traditionally used to purify VDAC from solubilized membranes. The results obtained in this work show that the chromatographic pass-through is highly enriched in VDAC2 and contains traces of VDAC3 and VDAC1. This result indicates that all VDAC isoforms solubilized in non-ionic detergents micelles have a similar behaviour toward the hydroxyapatite/celite chromatographic material, implying a similar structural architecture. This result also confirms previous information about the transcription levels in the testis, highlighting a reduced expression of VDAC1 in this tissue and the specific production of VDAC2 mRNA [34].

Functional characterization of native VDAC2

To our knowledge, this is the first report of the generation of enriched native VDAC2 protein**.** This gave us the opportunity to perform reconstitution experiments in the “black membrane” set up. When the VDAC was added to the artificial bilayer, the conductance of the membrane increased by several orders of magnitude. Its time course was similar to that described previously for VDAC1 of mitochondrial or bacterial origin [35-36].

The addition of purified bovine spermatozoa VDAC2 at very small concentrations allowed the resolution of step increases in membrane conductance. Many of the conductance steps had a single-channel conductance of about 3.5 nS in 1 M KCl. Very often small short-lived fluctuations were observed on top of the conductance steps. These fluctuations were absent for most mitochondrial VDAC (VDAC1) studied in the past. As demonstrated by the histogram a considerable number of

conductance steps had a lower single-channel conductance of about 1.5 nS. Channels with lower conductance were also observed for many mitochondrial VDAC but not as frequently as here. However, it is also possible that closing and re-opening events have some effect on the histograms because conductance of channel closure was generally smaller than that of the initial reconstitution of bovine spermatozoa VDAC.

Bovine spermatozoa VDAC was permeable for a variety of ions. Although a considerable influence of the type of ions on the pore conductance was found, the ratio between single channel conductance G and the bulk aqueous conductance varied less than a factor of two, i.e. the ions seemed to move within the pore in a manner similar to that in an aqueous environment. This finding suggests that VDAC2 forms a wide water-filled channel. On the other hand, the data show that the channels exhibit certain ion selectivity. The difference of the single channel conductance between KCH_3COOH and LiCl suggested that VDAC2 was anion-selective since the exchange of K^+ by the less mobile Li^+ had a relatively small effect on the single-channel conductance as compared to the replacement of Cl^- by the less mobile acetate anion (K^+ and Cl^- and Li^+ and acetate have the same aqueous mobility).

Zero-current membrane potential measurements performed to study the ion selectivity of bovine spermatozoa VDAC2 in more detail agreed with a small anion selectivity of the channel. Salt gradients were established across membranes containing 100 to 1000 channels into a membrane. The more diluted side of the membrane became negative which indicated preferential movement of chloride over potassium ions. The anion selectivity of the channel was, however, rather small as derived from the Goldman-Hodgkin-Katz equation [27]. Voltage-dependence experiments with bovine spermatozoa VDAC were performed under multi-channel conditions, i.e. many pores were reconstituted into the membrane. The voltage across the membrane was set to different potentials ranging from 10 mV to 100 mV and the membrane currents were monitored on the strip chart recorder. The initial current, i.e. the current immediately after application of the voltage, was a linear function of the applied membrane potential. For voltages larger than 20 mV the membrane current decayed exponentially to a smaller value. The maximum conductance decrease was observed at a voltage of about 70 mV. Higher potentials did not cause a further conductance decrease.

The functional characterization obtained with the native VDAC2 protein was compared with results obtained by Xu et al with recombinant mouse VDAC expressed in yeast and afterwards purified [12]. Recombinant mouse VDAC2 inserted easily into the phospholipid bilayer but the VDAC2 channels inserted in two conductance states: a higher conductance state and a lower conductance state. The authors claimed for the presence of two wholly distinct populations of VDAC2 channels, since the change from a lower to a higher conductance state was never observed, even in extended recordings of single channels [12]. These observations agree well with our data, which show a rather broad distribution of channels in the histogram of insertion events. The flickering of the traces obtained from bovine sperm VDAC2 is possibly due to the different source of the protein. Recombinant mouse VDAC2 expressed in yeast cells showed the same voltage dependence as the native protein.

Molecular analysis of native VDAC2

The chromatographed HTP/celite pass-through was subjected to molecular analysis by means of an extensive electrophoretic and proteomic study. In mono-dimensional SDS-PAGE 2-3 bands were found in the chromatographic eluate. The two major bands were identified as VDAC2 with western blot analysis. Arcelay et al found in spermatozoa extracts two separate bands stained with an anti-VDAC antibody, not specific for isoform 2 [37]. The bands found in 1D electrophoresis expanded in a complex pattern of about 10 spots in 2-D gels. Due to difference in the relative amount of the three isoforms, western blots with monospecific antibodies were used to detect the trace amount of VDAC1 and VDAC3 present in the gels. Limited proteolysis and sequencing of peptides of VDAC protein spots from the 2D gels yielded amino acid sequences matching with VDAC1, VDAC2 and VDAC3

proteins present in the public databases. However in the purified sperm VDAC protein mixture, six out of ten distinct main spots were VDAC2 while two faint, almost not detectable protein spots contained VDAC1 and one faint smear obviously consisted of VDAC3. Thus, in the HTP/celite pass-through of Triton X-100 solubilized spermatozoa, there was a clear predominance of VDAC2, while VDAC1 and VDAC3 appeared as a very small portion of "contaminating" VDACs in an enriched VDAC2 protein fraction. In particular VDAC2 originated five distinct spots with a well distinct pattern: they were focussed at two different molecular weights and at three different pIs, giving raise to a characteristic checkerboard distribution. Liberatori et al [38] found in guinea pig brain synaptosomes three spots corresponding to VDAC2, all with the same molecular mass but different pIs. Yamamoto et al [39] identified in rat liver mitochondria two spots as VDAC2, again with the same molecular masses. In both cases VDAC2 was the most acidic VDAC isoform, which we could confirm. In comparison with other proteomic studies we thus found in spermatozoa the presence of a row of two more spots, both with the same lower electrophoretic mobility but with *pI*s identical to those of other VDAC2 spots. This result raised the intriguing hypothesis of the expression of two VDAC2 sub-isoforms, with different polypeptide lengths, and with a pattern of similar post-translational modification. The first issue is justified by the evidence of alternative splicing that could add N-terminal sequences with different lengths to the β-barrel forming structure [30, 40]. The second issue was also justified by the observation that VDAC2 can be phosphorylated in various situations: changes in the isoelectric point of a protein indeed are often due to post-translational modifications. VDAC2 was found to be phosphorylated in guinea pig synaptosomes after hypoxia [38]. Distler et al showed that in VDAC2 Tyr-237 is phosphorylated [INSR site, 28]. Phosphorylation may have a relevant functional role in VDAC, since it can influence the activity of the pore as has previously been shown for VDAC1 in [41]. Phosphorylation may also induce conformational changes or could be involved in intracellular signalling. Very recently it was found that in the process of spermatozoa capacitation a VDAC protein was tyrosine-phosphorylated and this VDAC isoform identified as VDAC2 [with a sequence coverage of about 20%) [37].

Sequence coverage of VDAC2 migrating in the high molecular weight SDS band was about 98.6 %. In addition, mass spectrometric data revealed a sequence heterogeneity at level of the tryptic peptide T_{11}. In fact, the expected T_{11} was also accompanied by two modified T_{11}, carrying the amino acid substitutions T_{88} to L_{88} and A_{97} to Q_{97}, respectively. Instead, the characterization of the lower Mw VDAC2 was scant, allowing a sequence coverage of 71%. In this case it is worth to be noted that a large unidentified sequence corresponded to almost the whole sequence coded by exon 7 in the VDAC2 gene [30] and overlapped the largest undetermined rat liver VDAC2 peptide reported in [28]. It is possible that this sequence corresponds to a hot area of protein heterogeneity and, together with the amino acid substitutions, could explain the electrophoretic behaviour of the protein. A massive utilization of post-translational modification was not apparent from our results. We are presently engaged in the whole sequence determination of the lower VDAC2 band from bovine spermatozoa to answer the remaining structural questions.

VDACs in spermatozoa

Mammalian spermatozoa are highly differentiated haploid cells that are unable to synthesize proteins de novo. Therefore, most of the components found in mature spermatozoa are primarily formed in spermatids. Several genes are differentially expressed during sperm maturation giving rise to alternative transcripts, to different proteins and/or to different role in the mature spermatozoa [42].

The first clue of a role of VDAC in mammal spermatozoa was obtained by Sampson et al [14]. They produced mice lacking VDAC3 in their genome. These mice are healthy, but males are infertile. Although they have a normal sperm number, spermatozoa exhibit markedly reduced motility. When viewed by electron microscopy, 68% of VDAC3 deficient epididymal sperm axonemes (versus 9% of

wild type axonemes) have some structural aberration, most commonly loss of one outer doublet from the normal 9+2 microtubules doublet arrangement. Electron microscopy of spermatids in the testes revealed enlarged and abnormally shaped mitochondria along the midpiece. Infertility by sperm immotility may be a consequence of axonemal defects [14].

In addition to the data obtained in VDAC3 KO mice, it has been shown that also VDAC2 protein is present in testis [43-44]. mRNA analysis revealed the specific expression of VDAC2 in bovine testis; high levels of VDAC2 proteins were found in late spermatocytes, spermatids and spermatozoa. In contrast, VDAC1 was exclusively localized in Sertoli cells [43]. We have shown for the first time the extra-membranous localization of VDAC2 and VDAC3 in the ODF of the sperm flagellum [15]. ODF is a highly insoluble component of the midpiece and the principal piece of the sperm tail. It has been suggested that it can maintain the passive elastic structure and elastic recoil of the sperm flagellum and possibly also protect it from shearing forces during epididymal transport. The mitochondria in spermatozoa are in a very restricted cytoplasmic space in the midpiece where they can get in close proximity with the same ODF, the plasma membrane and the acrosomal membrane. For this reason in the sperm mitochondria there is a structural difference in the sides of mitochondria, as noticed with TEM [45]. It is thus tempting to speculate that the various VDAC isoforms may have different localizations in the spermatozoa, either in ODF or in mitochondria (where we could also suppose a specific sub-localization) or even in the plasma membrane, since the surface of spermatozoa can be strongly stained with fluorescent antibodies against VDAC2 [15, 37]. Solubilization with the non-ionic detergent Triton X-100 or with the harsh detergent SDS gave, indeed different patterns of solubilization of the VDAC isoforms in spermatozoa.

Tyrosine phosphorylation of specific proteins may have a regulatory effect on spermatozoa. It was found for the first time by Ficarro et al that VDAC may undergo such kind of modification in the sperm [44]. It was recently demonstrated that a limited set of proteins is specifically phosphorylated during sperm capacitiation, i.e. the process when the spermatozoa becomes competent for the egg fertilization: among them, not surprisingly, there is also VDAC2 [37]. It is not known what residue is modified.

These results raised even more intriguing questions. What is the distribution of VDAC proteins in the subcellular structures of spermatozoa? Is there any kind of specific maturation of VDAC isoforms (i.e. by transcriptional regulation or post-translational modification) during the spermatozoa differentiation and/or maturation, that can justify specific subcellular localizations or functions? Since the deficiency of VDAC3 causes axoneme structural impairment only in mature spermatozoa, is there any role of VDAC2 and VDAC3 in the development of the mature male germ cell?

Conclusions

In this work we have obtained, for the first time, a protein fraction from bovine spermatozoa highly enriched in native VDAC2. This has allowed us to characterize the molecular and functional features of this protein. Despite the presence of contaminating VDAC isoforms 1 and 3, the molecular characterization obtained with proteomic tools has allowed us to clearly trace the VDAC2. In the same way, the functional characterization of VDAC2 was only slightly affected by the presence of contaminating VDAC isoforms. This is because VDAC3 is essentially not active in planar bilayers [12] and VDAC1 is present in a very little amount and has distinguishable, not fully overlapping, features [12].

VDAC2, with a longer N-terminus, has the same electrophoretic mobility than VDAC1 [38] with the exception of the spermatozoa where it is specifically present with two electrophoretic mobilities. In addition its specific activity is much lower than VDAC1 [12]. In a retrospective view, taken all together, this information suggest that VDAC2 might have been a hidden contaminant of VDAC1 preparations claimed to be pure in the past. As described previously [38] VDAC2 is produced in lower

abundance than VDAC1 in every tissue with the exception of spermatozoa. The adoption of a source almost devoid of VDAC1 has allowed us to disclose the presence of VDAC2 and to highly enrich it. More experiments are still needed to detail in deep the properties of this important VDAC isoform in a cellular context.

Acknowledgment: The authors wish to thank Ms. Simone Becker, Center of Dermatology and Andrology, Giessen, and Bettina Schiffler, Lehrstuhl für Biotechnologie, Universität Würzburg for expert technical assistance.

REFERENCES

1. Schein, S. J., Colombini, M., Finkelstein, A. (1976) Reconstitution in planar lipid bilayers of a voltage-dependent anion-selective channel obtained from paramecium mitochondria. J. Membr. Biol. **30**, 99-120
2. Benz, R. (1994) Permeation of hydrophilic solutes through mitochondrial outer membranes: review on mitochondrial porins. Biochim. Biophys. Acta **1197**, 167-196
3. Benz, R. (2004) Structure and function of mitochondrial (eukaryotic) porins. In Bacterial and eukaryotic porins. Structure, function, mechanism. (Benz, R. ed) pp 259-284, Wiley-VCH: Weinheim
4. Shoshan-Barmatz, V., Israelson, A., Brdiczka, D., Sheu, S. S. (2006) The voltage-dependent anion channel (VDAC): function in intracellular signalling, cell life and cell death. Curr. Pharm. Des **12**, 2249-2270
5. Lemasters, J.J. (2007) Modulation of mitochondrial membrane permeability in pathogenesis, autophagy and control of metabolism. Journal of Gastroenterology and Hepatology **22** Suppl. 1; S31–S37
6. Linden, M., Karlsson, G. (1996) Identification of porin as a binding site for MAP2. Biochem. Biophys. Res Commun. **218**, 833-836
7. Schwarzer, C., Barnikol-Watanabe, S., Thinnes, F. P., Hilschmann, N. (2002) Voltage-dependent anion-selective channel (VDAC) interacts with the dynein light chain Tctex1 and the heat-shock protein PBP74. Int. J. Biochem. Cell Biol. **34,** 1059-1070
8. Xu, X., Forbes, J. G., Colombini, M. (2001) Actin modulates the gating of Neurospora crassa VDAC. J. Membr. Biol. **180**, 73-81
9. Bathori, G., Parolini, I., Szabo, I., Tombola, F., Messina, A., Oliva, M., Sargiacomo, M., De Pinto, V., Zoratti, M. (2000) Extramitochondrial porin: facts and hypotheses. J. Bioenerg. Biomembr. **32**, 79-89
10. De Pinto, V., Reina, S., Guarino, F., Messina, A. (2008) Structure of the Voltage Dependent Anion Channel: state of the art J. Bioenerg. Biomembr. **40**, 139-147
11. Sampson, M.J., Lovell, R.S. and Craigen, W.J. (1997) The murine voltage-dependent anion channel gene family. Conserved structure and function. J. Biol. Chem. **272**, 18966-18973
12. Xu, X., Decker, W., Sampson, M.J., Craigen, W.J. and Colombini, M. (1999) Mouse VDAC isoforms expressed in yeast: channel properties and their roles in mitochondrial outer membrane permeability. J. Membr. Biol. **170**, 89-102
13. Cheng, E.H., Sheiko, T.V., Fisher, J.K., Craigen, W.J. and Korsmeyer, S.J. (2003) VDAC2 inhibits BAK activation and mitochondrial apoptosis. Science **301**, 513-517
14. Sampson, M.J., Decker, W.K., Beaudet, A.L., Ruitenbeek, W, Armstrong, D., Hicks, M.J. and Craigen WJ. (2001) Immotile sperm and infertility in mice lacking mitochondrial voltage-dependent anion channel type 3. J. Biol. Chem. **276**, 39206-12
15. Hinsch, K.D., De Pinto, V., Aires, V.A., Schneider, X., Messina, A. and Hinsch, E. (2004) Voltage-dependent anion selective channels VDAC2 and VDAC3 are abundant proteins in bovine outer dense fibers, a cytoskeletal component of the sperm flagellum. J. Biol. Chem. **279**, 15281-15288
16. Anflous, K., Craigen, W. J. (2004) Mitochondrial porins in mammals: insights into functional roles from mutant mice and cells. In Bacterial and eukaryotic porins. Structure, function, mechanism. (Benz, R. ed) pp 285-305 WILEY-VCH, Weinheim
17. Chandra, D., Choy, G., Daniel, P.T., Tang, D.G. (2005) Bax-dependent regulation of Bak by voltage-dependent anion channel 2. J. Biol. Chem. **280**, 19051-61
18. Yagoda, N., von Rechenberg, M., Zaganjor, E., Bauer, A.J., Yang, W.S., Fridman, D.J., Wolpaw, A.J., Smukste, I., Peltier, J.M., Boniface, J.J., Smith, R., Lessnick, S.L., Sahasrabudhe, S., Stockwell,

B.R. (2007) RAS-RAF-MEK-dependent oxidative cell death involving voltage-dependent anion channels. Nature **447**, 864-8
19. Triphan, X., Menzel, V.A., Petrunkina, A.M., Cassará, M.C., Wemheuer, W., Hinsch, K.D., Hinsch, E. (2008) Localisation and function of voltage-dependent anion channels (VDAC) in bovine spermatozoa. Pflugers Arch. **455**, 677-86
20. Guarino, F., Specchia, V., Zapparoli, G., Messina, A., Aiello, R., Bozzetti, M. P., De Pinto, V. (2006) Expression and localization in spermatozoa of the mitochondrial porin isoform 2 in Drosophila melanogaster. Biochem. Biophys. Res. Commun. **346**, 665-670
21. De Pinto, V., Prezioso, G., Palmieri, F. (1987) A simple and rapid method for the purification of the mitochondrial porin from mammalian tissues. Biochim. Biophys. Acta **905**, 499-450
22. Laemmli, U. K. (1970) Cleavage of structural proteins during assembly of the head of bacteriophage T4. Nature **227**, 680-685
23. Hinsch, E., Hinsch, K. D. (1996) Generation of antisera against mouse and human synthetic ZP3 peptides. Andrologia **28** Suppl 1, 9-14
24. Shevchenko, A., Wilm, M., Vorm, O., Mann, M. (1996) Mass spectrometric sequencing of proteins silver-stained polyacrylamide gels. Anal. Chem. **68**, 850-858
25. Gobom, J., Nordhoff, E., Mirgorodskaya, E., Ekman, R., Roepstorff, P. (1999) Sample purification and preparation technique based on nano-scale reversed-phase columns for the sensitive analysis of complex peptide mixtures by matrix-assisted laser desorption/ionization mass spectrometry. J. Mass Spectrom. **34**, 105-116
26. Benz, R., Janko, K., Boos, W., Lauger, P. (1978) Formation of large, ion-permeable membrane channels by the matrix protein (porin) of Escherichia coli. Biochim. Biophys. Acta **511**, 305-319
27. Benz, R., Janko, K., Lauger, P. (1979) Ionic selectivity of pores formed by the matrix protein (porin) of Escherichia coli. Biochim. Biophys. Acta **551**, 238-247
28. Distler, A.M., Kerner, J., Peterman, S.M., Hoppel, C.L. (2006) A targeted proteomic approach for the analysis of rat liver mitochondrial outer membrane proteins with extensive sequence coverage. Anal. Biochem. **356**, 18-29
29. Lindén, M., Gellerfors, P., Nelson, B.D. (1982) Pore protein and the hexokinase-binding protein from the outer membrane of rat liver mitochondria are identical. FEBS Lett. **141**, 189-92
30. De Pinto, V., Messina A., (2004) Gene family expression and multitopological localization of eukaryotic porin/VDAC - Intracellular trafficking and alternative splicing of mitochondrial porin/VDAC in Bacterial and eukaryotic porins. Structure, function, mechanism. (Benz, R., ed) pp 309-337 WILEY-VCH, Weinheim
31. Yoo, B.C., Vlkolinsky, R., Engidawork, E., Cairns, N., Fountoulakis, M., Lubec, G. (2001) Differential expression of molecular chaperones in brain of patients with Down syndrome. Electrophoresis **22**, 1233-41
32. Shinohara, Y., Ishida, T., Hino, M., Yamazaki, N., Baba, Y., Terada, H. (2000) Characterization of porin isoforms expressed in tumor cells. Eur. J. Biochem. **267**, 6067-73
33. Hastie, C., Saxton, M., Akpan, A., Cramer, R., Masters, J.R., Naaby-Hansen, S. (2005) Combined affinity labelling and mass spectrometry analysis of differential cell surface protein expression in normal and prostate cancer cells. Oncogene **24**, 5905-13
34. Sampson, M.J., Lovell, R.S., Craigen, W.J. (1996) Isolation, characterization, and mapping of two mouse mitochondrial voltage-dependent anion channel isoforms. Genomics **33**, 283-288
35. Roos, N., Benz, R., Brdiczka, D. (1982) Identification and characterization of the pore-forming protein in the outer membrane of rat liver mitochondria. Biochim. Biophys. Acta **686**, 204-214
36. Troll, H., Malchow, D., Müller-Taubenberger, A., Humbel, B., Lottspeich, F., Ecke, M., Gerisch, G., Schmid, A., Benz, R. (1992) Purification, functional characterization, and cDNA sequencing of mitochondrial porin from Dictyostelium discoideum. J. Biol. Chem. **267**, 21072-9

37. Arcelay, E., Salicioni, A.M., Wertheimer, E., Visconti, P.E. (2008) Identification of proteins undergoing tyrosine phosphorylation during mouse sperm capacitation. Int. J. Dev. Biol. **52**, 463-472
38. Liberatori, S., Canas, B., Tani, C., Bini, L., Buonocore, G., Godovac-Zimmermann, J., Mishra, O.P., Delivoria-Papadopoulos, M., Bracci, R., Pallini, V. (2004) Proteomic approach to the identification of voltage-dependent anion channel protein isoforms in guinea pig brain synaptosomes. Proteomics **4**, 1335-40
39. Yamamoto, T., Yamada, A., Watanabe, M., Yoshimura, Y., Yamazaki, N., Yoshimura, Y., Yamauchi, T., Kataoka, M., Nagata, T., Terada, H., Shinohara, Y. (2006) VDAC1, having a shorter N-terminus than VDAC2 but showing the same migration in an SDS-polyacrylamide gel, is the predominant form expressed in mitochondria of various tissues. J. Proteome Res. **5**, 3336-44
40. Ha, H., Hajek, P., Bedwell, D.M., Burrows, P.D. (1993) A mitochondrial porin cDNA predicts the existence of multiple human porins. J. Biol. Chem. **268**, 12143-9
41. Bera, A.K., Ghosh, S., Das, S. (1995) Mitochondrial VDAC can be phosphorylated by cyclic AMP-dependent protein kinase. Biochem. Biophys. Res Commun. **209**, 213-217
42. Steger, K. (1999) Transcriptional and translational regulation of gene expression in haploid spermatids Anat Embryol (Berl) **199**, 471–487
43. Hinsch, K.D., Asmarinah, Hinsch, E., Konrad, L. (2001) VDAC2 (porin-2) expression pattern and localization in the bovine testis. Biochim. Biophys. Acta **1518**, 329-333
44. Ficarro, S., Chertihin, O., Westbrook, V.A., White, F., Jayes, F., Kalab, P., Marto, J.A., Shabanowitz, J., Herr, J.C., Hunt, D.F., Visconti, P.E. (2003) Phosphoproteome analysis of capacitated human sperm. Evidence of tyrosine phosphorylation of a kinase-anchoring protein 3 and valosin-containing protein/p97 during capacitation. J. Biol. Chem. **278**, 11579-11589
45. Olson, G.E., Winfrey, V.P. (1985) Structure of membrane domains and matrix components of the bovine acrosome. J. Ultrastruct. Res. **90**, 9-25

LEGENDS TO FIGURES

Figure 1. A. 12% SDS-PAGE of protein preparation from bovine spermatozoa after 2% Triton X-100 extraction (TX, $25x10^6$ spermatozoa per lane) and hydroxyapatite/celite purification (H/C, $165x10^6$ spermatozoa per lane). After separation, proteins were stained by Coomassie. M: Molecular weight markers (on the left the molecular masses are indicated). The arrows show the three bands eluted. **B.** The sequences of the upper band of VDAC2 (band I) and of the lower band II as found in mono-dimensional SDS-PAGE were obtained by MALDI-TOFMS and RP-HPLC/ESI-MS/MS data of the in-gel tryptic digest of the two bands. In bold and underlined are the sequences that have not been covered by the mass spectrometric analysis. Underlined in the lane of VDAC2 band I is the tryptic peptide T11 (76-->107). Two variants, in addition to the expected sequence, were found in the spectra from the VDAC2 band I peptide T11: a T-->L substitution at position 88 and a A-->Q substitution at position 97.

Figure 2. Separation of Coomassie blue staining of the hydroxyapatite/celite purified proteins from bovine spermatozoa separated by 2-DE. The marked spots were excised and analyzed by MALDI-TOF/ MS.

Figure 3. Immuno staining of hydroxyapatite/celite purified proteins from bovine spermatozoa with anti-VDAC antibodies. **A**: anti-VDAC1 antibodies (AS P1/6). **B**: anti-VDAC2 antibodies (AS P2/45). **C**: anti-VDAC3 antibodies (AS P3/31). Proteins were separated by 2-DE. Data are representative for at least three separate experiments.

Figure 4. Stepwise increase of the membrane conductance (expressed in nS) after the addition of enriched VDAC2 protein from bovine sperm to a black lipid bilayer membrane given as a function of time. The membrane was formed from diphytanoylphosphatidylcholine/n-decane. The aqueous phase contained 1 M KCl, pH 8 and about 10 ng/ml protein added to the cis-side of the membrane. The applied membrane potential was 10 mV; T = 20°C.

Figure 5. Histogram of the probability for the occurrence of a given conductivity unit observed with membranes formed of diphytanoylphosphatidylcholine/*n*-decane in the presence of 10 ng/ml enriched VDAC2 protein. The ordinate shows the percentage of single-channel events observed for a given conductance increment. It was calculated by dividing the number of events with a given conductance increment by the total number of conductance fluctuations. The overall average single-channel conductance was 2.25 nS for 148 single-channel events. The average single-channel conductance of left side maximum was about 1.5 nS and that of the right side was about 3.3 nS. The aqueous phase contained 1 M KCl, pH 6. The voltage applied was 10 mV, and T = 20 °C.

Figure 6. A. Study of the voltage-dependence of VDAC2 protein. 100 ng/ml protein was added to the cis-side of a diphytanoylphosphatidylcholine/*n*-decane membrane and the reconstitution of the channels was followed for about 30 min. Then increasing positive (40 to 70 mV; upper traces) and negative voltages (-40 to -70 mV; lower traces) were applied to the cis-side of the membrane and the membrane current was measured as a function of the time. The aqueous phase contained 1 M KCl, pH 6; T = 20°C. **B. Voltage dependence G/G_0 of purified VDAC2 measured as a function of the applied voltage (V_m).** Ratio of the conductance G at a given membrane potential (V_m) divided by the conductance G_o at 10 mV as a function of the membrane potential V_m. The full squares represent the mean of 4 measurements, in which about 100 ng/ml enriched VDAC2 from bovine sperm was added

to the cis-side of membranes. The aqueous phase contained 1 M KCl, pH 7.0. The membranes were formed from diphytanoylphosphatidylcholine/*n*-decane. T = 20°C.

Bioscience Reports Immediate Publication. Published on 31 Oct 2008 as manuscript BSR20080123

Figure 1 **Aires et al**

A

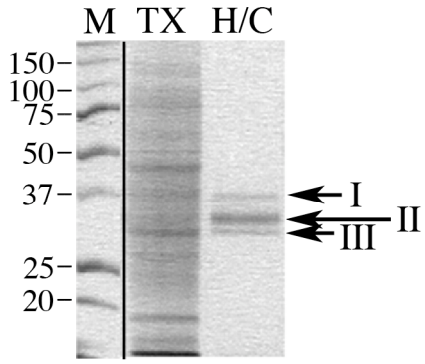

B

```
VDAC2 band I   MATYGQNCARPMCIPPSYADLGKAARDIFNKGFGFGLVKLDVKTKSCSGV  50
VDAC2 band II  MATYGQNCARPMCIPPSYADLGKAARDIFNKGFGFGLVKLDVKTKSCSGV  50

                                                  L          Q
VDAC2 band I   EFSTSGSSNTDTGKVTGTLETKYKWCEYGLTFTEKWNTDNTLGTEIAIED 100
VDAC2 band II  EFSTSGSSNTDTGKVTGTLETKYKWCEYGLTFTEKWNTDNTLGTEIAIED 100

VDAC2 band I   QICQGLKLTFDTTFSPNTGKKSGKIKSSYKRECINLGCDVDFDFAGPAIH 150
VDAC2 band II  QICQGLKLTFDTTFSPNTGKKSGKIKSSYKRECINLGCDVDFDFAGPAIH 150

VDAC2 band I   GSAVFGYEGWLAGYQMTFDSAKSKLTRNNFAVGYRTGDFQLHTNVNDGTE 200
VDAC2 band II  GSAVFGYEGWLAGYQMTFDSAKSKLTRNNFAVGYRTGDFQLHTNVNDGTE 200

VDAC2 band I   FGGSIYQKVCEDLDTSVNLAWTSGTNCTRFGIAAKYQLDPTASISAKVNN 250
VDAC2 band II  FGGSIYQKVCEDLDTSVNLAWTSGTNCTRFGIAAKYQLDPTASISAKVNN 250

VDAC2 band I   SSLIGVGYTQTLRPGVKLTLSALVDGKSINAGGHKLGLALELEA 294
VDAC2 band II  SSLIGVGYTQTLRPGVKLTLSALVDGKSINAGGHKLGLALELEA 294
```

Bioscience Reports Immediate Publication. Published on 31 Oct 2008 as manuscript BSR20080123

Figure 2 **Aires et al**

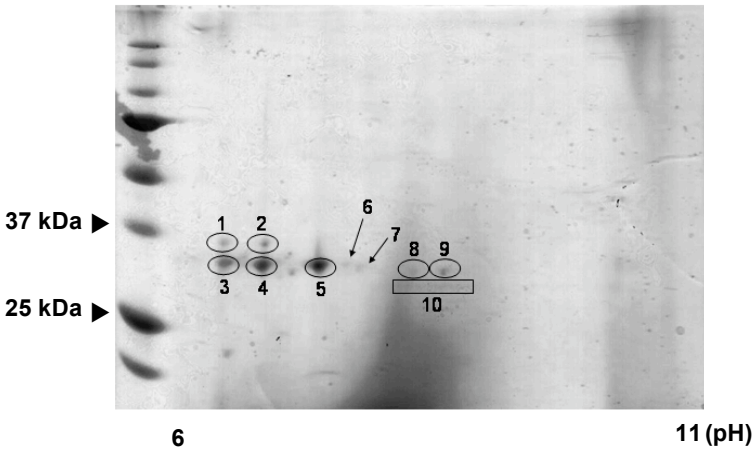

Figure 3 **Aires et al**

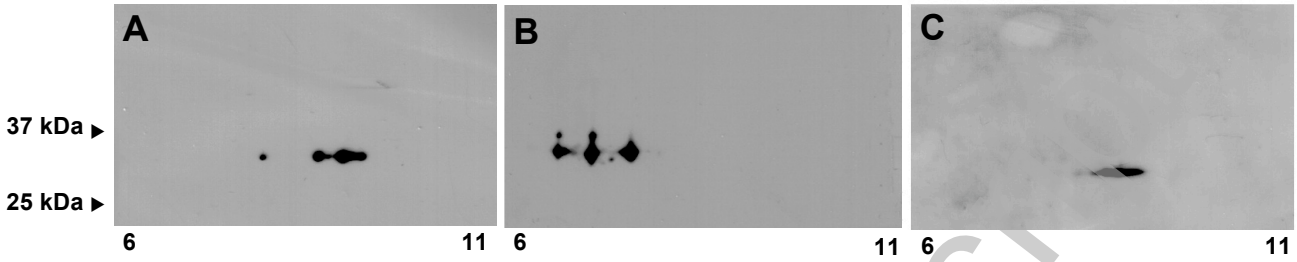

Bioscience Reports Immediate Publication. Published on 31 Oct 2008 as manuscript BSR20080123

Figure 4 **Aires et al**

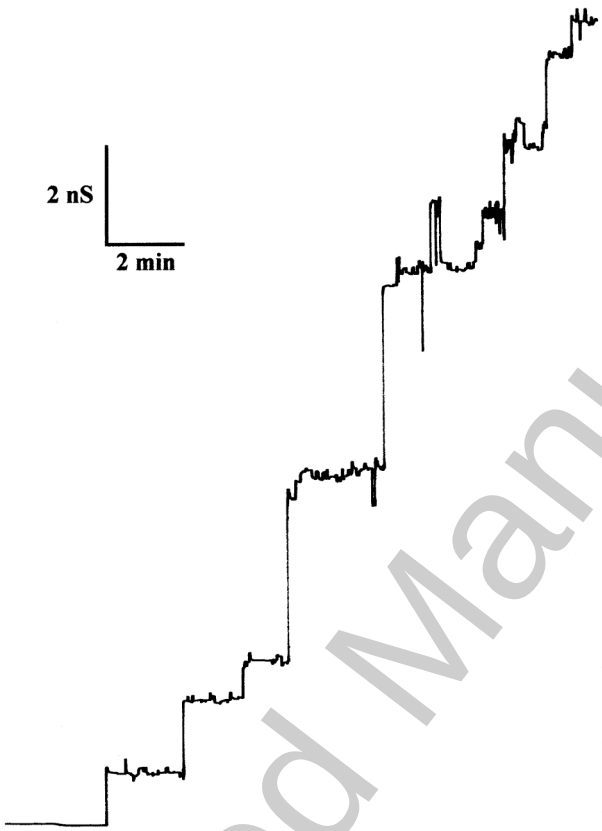

Figure 5 **Aires et al.**

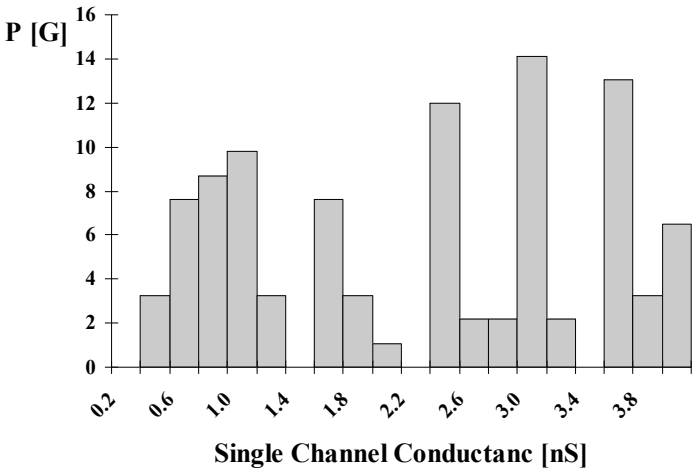

Figure 6 **Aires et al.**

A

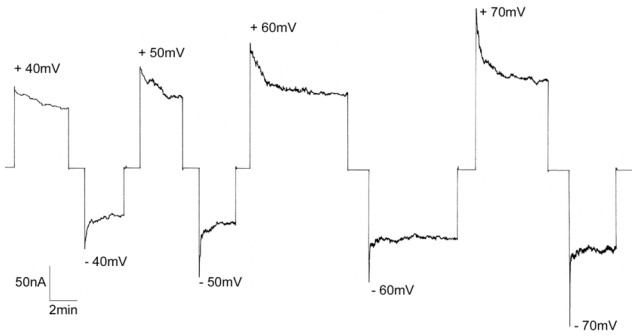

B

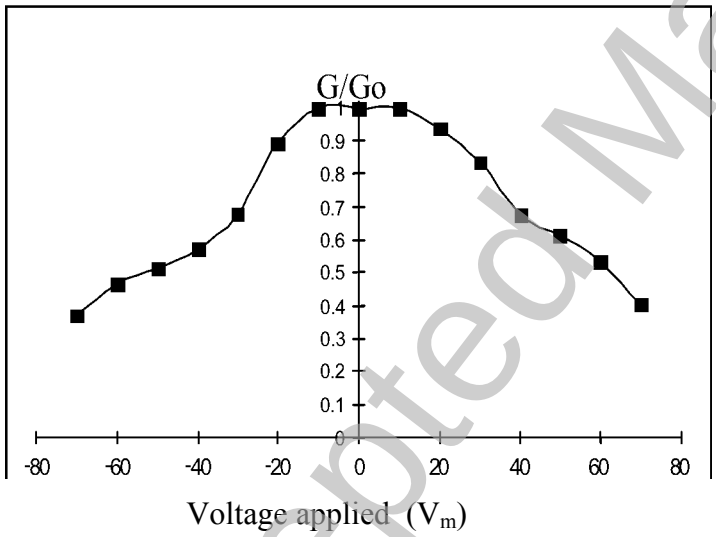

Table 1. Peptides identified by MALDI-TOF/MS of hydroxyapatite/celite purified proteins from bovine spermatozoa

Gel spot number	Protein	Protein coverage	MW	pI	Accession number	MOWSE score*	No. of peptides matched
1	VDAC2_BOVIN	52 %	32113	7.48	P68002	120	12
2	VDAC2_BOVIN	72 %	32113	7.48	P68002	118	20
3	VDAC2_BOVIN	69 %	32113	7.48	P68002	192	17
4	VDAC2_BOVIN	69 %	32113	7.48	P68002	192	17
5	VDAC2_BOVIN	69 %	32113	7.48	P68002	212	18
6	VDAC2_BOVIN	59 %	32113	7.48	P68002	117	12
8	VDAC1_BOVIN	61 %	30705	8.63	P45879	132	13
9	VDAC1_BOVIN	63 %	30705	8.63	P45879	164	15
10	VDAC3_BOVIN	40 %	31062	8.95	Q9MZ13	97	12

*Protein scores greater than 60 are significant ($p<0.05$).

Table 2. Average single-channel conductance, G, of enriched VDAC2 from bovine sperm in different salt solutions.

Salt	Concentration C [M]	Single channel conductance G [nS]	
		Left hand maximum	Right hand maximum
LiCl	1.0	1.0	2.6
KAc	1.0	1.0	-
KCl	1.0	1.5	3.3
	0.3	0.6	-
	01	0.5	-

The membranes were formed of 1% PC dissolved in n-decane. The aqueous solutions were used unbuffered and had a pH of 6, unless otherwise indicated. The applied voltage was 10 mV and the temperature was 20°C. The average single-channel conductance, G, was calculated from at least 80 single events derived from measurements of at least four individual membranes. Please note that in certain cases two maxima were observed (see Figure 5).